



Title	Search for a light exotic particle in J/ψ radiative decays
-------	---

Search for a light exotic particle in J/ψ radiative decays

M. Ablikim,¹ M. N. Achasov,⁵ D. J. Ambrose,⁴⁰ F. F. An,¹ Q. An,⁴¹ Z. H. An,¹ J. Z. Bai,¹ Y. Ban,²⁷ J. Becker,² N. Berger,¹ M. B. Bertani,¹⁸ J. M. Bian,³⁹ E. Boger,^{20,*} O. Bondarenko,²¹ I. Boyko,²⁰ R. A. Briere,³ V. Bytev,²⁰ X. Cai,¹ A. C. Calcaterra,¹⁸ G. F. Cao,¹ J. F. Chang,¹ G. Chelkov,^{20,*} G. Chen,¹ H. S. Chen,¹ J. C. Chen,¹ M. L. Chen,¹ S. J. Chen,²⁵ Y. Chen,¹ Y. B. Chen,¹ H. P. Cheng,¹⁴ Y. P. Chu,¹ D. Cronin-Hennessy,³⁹ H. L. Dai,¹ J. P. Dai,¹ D. Dedovich,²⁰ Z. Y. Deng,¹ A. Denig,¹⁹ I. Denysenko,^{20,†} M. Destefanis,⁴⁴ W. M. Ding,²⁹ Y. Ding,²³ L. Y. Dong,¹ M. Y. Dong,¹ S. X. Du,⁴⁷ J. Fang,¹ S. S. Fang,¹ L. Fava,^{44,‡} F. Feldbauer,² C. Q. Feng,⁴¹ R. B. Ferroli,¹⁸ C. D. Fu,¹ J. L. Fu,²⁵ Y. Gao,³⁶ C. Geng,⁴¹ K. Goetzen,⁷ W. X. Gong,¹ W. Gradl,¹⁹ M. Greco,⁴⁴ M. H. Gu,¹ Y. T. Gu,⁹ Y. H. Guan,⁶ A. Q. Guo,²⁶ L. B. Guo,²⁴ Y. P. Guo,²⁶ Y. L. Han,¹ X. Q. Hao,¹ F. A. Harris,³⁸ K. L. He,¹ M. He,¹ Z. Y. He,²⁶ T. Held,² Y. K. Heng,¹ Z. L. Hou,¹ H. M. Hu,¹ J. F. Hu,⁶ T. Hu,¹ B. Huang,¹ G. M. Huang,¹⁵ J. S. Huang,¹² X. T. Huang,²⁹ Y. P. Huang,¹ T. Hussain,⁴³ C. S. Ji,⁴¹ Q. Ji,¹ X. B. Ji,¹ X. L. Ji,¹ L. K. Jia,¹ L. L. Jiang,¹ X. S. Jiang,¹ J. B. Jiao,²⁹ Z. Jiao,¹⁴ D. P. Jin,¹ S. Jin,¹ F. F. Jing,³⁶ N. Kalantar-Nayestanaki,²¹ M. Kavatsyuk,²¹ W. Kuehn,³⁷ W. Lai,¹ J. S. Lange,³⁷ J. K. C. Leung,³⁵ C. H. Li,¹ Cheng Li,⁴¹ Cui Li,⁴¹ D. M. Li,⁴⁷ F. Li,¹ G. Li,¹ H. B. Li,¹ J. C. Li,¹ K. Li,¹⁰ Lei Li,¹ N. B. Li,²⁴ Q. J. Li,¹ S. L. Li,¹ W. D. Li,¹ W. G. Li,¹ X. L. Li,²⁹ X. N. Li,¹ X. Q. Li,²⁶ X. R. Li,^{1,28} Z. B. Li,³³ H. Liang,⁴¹ Y. F. Liang,³¹ Y. T. Liang,³⁷ G. R. Liao,³⁶ X. T. Liao,¹ B. J. Liu,¹ B. J. Liu,³⁴ C. L. Liu,³ C. X. Liu,¹ C. Y. Liu,¹ F. H. Liu,³⁰ Fang Liu,¹ Feng Liu,¹⁵ H. Liu,¹ H. B. Liu,⁶ H. H. Liu,¹³ H. M. Liu,¹ H. W. Liu,¹ J. P. Liu,⁴⁵ K. Liu,²⁷ K. Liu,⁶ K. Y. Liu,²³ S. B. Liu,⁴¹ X. Liu,²² X. H. Liu,¹ Y. B. Liu,²⁶ Yong Liu,¹ Z. A. Liu,¹ Zhiqiang Liu,¹ Zhiqing Liu,¹ H. Loehner,²¹ G. R. Lu,¹² H. J. Lu,¹⁴ J. G. Lu,¹ Q. W. Lu,³⁰ X. R. Lu,⁶ Y. P. Lu,¹ C. L. Luo,²⁴ M. X. Luo,⁴⁶ T. Luo,³⁸ X. L. Luo,¹ M. Lv,¹ C. L. Ma,⁶ F. C. Ma,²³ H. L. Ma,¹ Q. M. Ma,¹ S. Ma,¹ T. Ma,¹ X. Y. Ma,¹ Y. Ma,¹¹ F. E. Maas,¹¹ M. Maggiora,⁴⁴ Q. A. Malik,⁴³ H. Mao,¹ Y. J. Mao,²⁷ Z. P. Mao,¹ J. G. Messchendorp,²¹ J. Min,¹ T. J. Min,¹ R. E. Mitchell,¹⁷ X. H. Mo,¹ C. Morales,¹¹ C. Motzko,² N. Yu. Muchnoi,⁵ Y. Nefedov,²⁰ I. B. Nikolaev,⁵ Z. Ning,¹ S. L. Olsen,²⁸ Q. Ouyang,¹ S. P. Pacetti,^{18,§} J. W. Park,²⁸ M. Pelizaeus,³⁸ K. Peters,⁷ J. L. Ping,²⁴ R. G. Ping,¹ R. Poling,³⁹ E. Prencipe,¹⁹ C. S. J. Pun,³⁵ M. Qi,²⁵ S. Qian,¹ C. F. Qiao,⁶ X. S. Qin,¹ Y. Qin,²⁷ Z. H. Qin,¹ J. F. Qiu,¹ K. H. Rashid,⁴³ G. Rong,¹ X. D. Ruan,⁹ A. Sarantsev,^{20,||} J. Schulze,² M. Shao,⁴¹ C. P. Shen,^{38,¶} X. Y. Shen,¹ H. Y. Sheng,¹ M. R. Shepherd,¹⁷ X. Y. Song,¹ S. Spataro,⁴⁴ B. Spruck,³⁷ D. H. Sun,¹ G. X. Sun,¹ J. F. Sun,¹² S. S. Sun,¹ X. D. Sun,¹ Y. J. Sun,⁴¹ Y. Z. Sun,¹ Z. J. Sun,¹ Z. T. Sun,⁴¹ C. J. Tang,³¹ X. Tang,¹ E. H. Thorndike,⁴⁰ H. L. Tian,¹ D. Toth,³⁹ M. U. Ulrich,³⁷ G. S. Varner,³⁸ B. Wang,⁹ B. Q. Wang,²⁷ K. Wang,¹ L. L. Wang,⁴ L. S. Wang,¹ M. Wang,²⁹ P. Wang,¹ P. L. Wang,¹ Q. Wang,¹ Q. J. Wang,¹ S. G. Wang,²⁷ X. F. Wang,¹² X. L. Wang,⁴¹ Y. D. Wang,⁴¹ Y. F. Wang,¹ Y. Q. Wang,²⁹ Z. Wang,¹ Z. G. Wang,¹ Z. Y. Wang,¹ D. H. Wei,⁸ P. Weidenkaff,¹⁹ Q. G. Wen,⁴¹ S. P. Wen,¹ M. W. Werner,³⁷ U. Wiedner,² L. H. Wu,¹ N. Wu,¹ S. X. Wu,⁴¹ W. Wu,²⁶ Z. Wu,¹ L. G. Xia,³⁶ Z. J. Xiao,²⁴ Y. G. Xie,¹ Q. L. Xiu,¹ G. F. Xu,¹ G. M. Xu,²⁷ H. Xu,¹ Q. J. Xu,¹⁰ X. P. Xu,³² Y. Xu,²⁶ Z. R. Xu,⁴¹ F. Xue,¹⁵ Z. Xue,¹ L. Yan,⁴¹ W. B. Yan,⁴¹ Y. H. Yan,¹⁶ H. X. Yang,¹ T. Yang,⁹ Y. Yang,¹⁵ Y. X. Yang,⁸ H. Ye,¹ M. Ye,¹ M. H. Ye,⁴ B. X. Yu,¹ C. X. Yu,²⁶ J. S. Yu,²² S. P. Yu,²⁹ C. Z. Yuan,¹ W. L. Yuan,²⁴ Y. Yuan,¹ A. A. Zafar,⁴³ A. Z. Zallo,¹⁸ Y. Zeng,¹⁶ B. X. Zhang,¹ B. Y. Zhang,¹ C. C. Zhang,¹ D. H. Zhang,¹ H. H. Zhang,³³ H. Y. Zhang,¹ J. Zhang,²⁴ J. Q. Zhang,¹ J. W. Zhang,¹ J. Y. Zhang,¹ J. Z. Zhang,¹ L. Zhang,²⁵ S. H. Zhang,¹ T. R. Zhang,²⁴ X. J. Zhang,¹ X. Y. Zhang,²⁹ Y. Zhang,¹ Y. H. Zhang,¹ Y. S. Zhang,⁹ Z. P. Zhang,⁴¹ Z. Y. Zhang,⁴⁵ G. Zhao,¹ H. S. Zhao,¹ Jingwei Zhao,¹ K. X. Zhao,²⁴ Lei Zhao,⁴¹ Ling Zhao,¹ M. G. Zhao,²⁶ Q. Zhao,¹ S. J. Zhao,⁴⁷ T. C. Zhao,¹ X. H. Zhao,²⁵ Y. B. Zhao,¹ Z. G. Zhao,⁴¹ A. Zhemchugov,^{20,*} B. Zheng,⁴² J. P. Zheng,¹ Y. H. Zheng,⁶ Z. P. Zheng,¹ B. Zhong,¹ J. Zhong,² L. Zhou,¹ X. K. Zhou,⁶ X. R. Zhou,⁴¹ C. Zhu,¹ K. Zhu,¹ K. J. Zhu,¹ S. H. Zhu,¹ X. L. Zhu,³⁶ X. W. Zhu,¹ Y. M. Zhu,²⁶ Y. S. Zhu,¹ Z. A. Zhu,¹ J. Zhuang,¹ B. S. Zou,¹ J. H. Zou,¹ and J. X. Zuo¹

(BESIII Collaboration)

¹*Institute of High Energy Physics, Beijing 100049, People's Republic of China*²*Bochum Ruhr-University, 44780 Bochum, Germany*³*Carnegie Mellon University, Pittsburgh, Pennsylvania 15213, USA*⁴*China Center of Advanced Science and Technology, Beijing 100190, People's Republic of China*⁵*G. I. Budker Institute of Nuclear Physics Siberian Branch of Russian Academy of Sciences (BINP), Novosibirsk 630090, Russia*⁶*Graduate University of Chinese Academy of Sciences, Beijing 100049, People's Republic of China*⁷*GSI Helmholtzcentre for Heavy Ion Research GmbH, D-64291 Darmstadt, Germany*⁸*Guangxi Normal University, Guilin 541004, People's Republic of China*⁹*GuangXi University, Nanning 530004, People's Republic of China*¹⁰*Hangzhou Normal University, Hangzhou 310036, People's Republic of China*

- ¹¹Helmholtz Institute Mainz, J.J. Becherweg 45, D 55099 Mainz, Germany
¹²Henan Normal University, Xinxiang 453007, People's Republic of China
¹³Henan University of Science and Technology, Luoyang 471003, People's Republic of China
¹⁴Huangshan College, Huangshan 245000, People's Republic of China
¹⁵Huazhong Normal University, Wuhan 430079, People's Republic of China
¹⁶Hunan University, Changsha 410082, People's Republic of China
¹⁷Indiana University, Bloomington, Indiana 47405, USA
¹⁸INFN Laboratori Nazionali di Frascati, Frascati, Italy
¹⁹Johannes Gutenberg University of Mainz, Johann-Joachim-Becher-Weg 45, 55099 Mainz, Germany
²⁰Joint Institute for Nuclear Research, 141980 Dubna, Russia
²¹KVI/University of Groningen, 9747 AA Groningen, The Netherlands
²²Lanzhou University, Lanzhou 730000, People's Republic of China
²³Liaoning University, Shenyang 110036, People's Republic of China
²⁴Nanjing Normal University, Nanjing 210046, People's Republic of China
²⁵Nanjing University, Nanjing 210093, People's Republic of China
²⁶Nankai University, Tianjin 300071, People's Republic of China
²⁷Peking University, Beijing 100871, People's Republic of China
²⁸Seoul National University, Seoul, 151-747 Korea
²⁹Shandong University, Jinan 250100, People's Republic of China
³⁰Shanxi University, Taiyuan 030006, People's Republic of China
³¹Sichuan University, Chengdu 610064, People's Republic of China
³²Soochow University, Suzhou 215006, China
³³Sun Yat-Sen University, Guangzhou 510275, People's Republic of China
³⁴The Chinese University of Hong Kong, Shatin, N.T., Hong Kong
³⁵The University of Hong Kong, Pokfulam, Hong Kong
³⁶Tsinghua University, Beijing 100084, People's Republic of China
³⁷Universitaet Giessen, 35392 Giessen, Germany
³⁸University of Hawaii, Honolulu, Hawaii 96822, USA
³⁹University of Minnesota, Minneapolis, Minnesota 55455, USA
⁴⁰University of Rochester, Rochester, New York 14627, USA
⁴¹University of Science and Technology of China, Hefei 230026, People's Republic of China
⁴²University of South China, Hengyang 421001, People's Republic of China
⁴³University of the Punjab, Lahore-54590, Pakistan
⁴⁴University of Turin and INFN, Turin, Italy
⁴⁵Wuhan University, Wuhan 430072, People's Republic of China
⁴⁶Zhejiang University, Hangzhou 310027, People's Republic of China
⁴⁷Zhengzhou University, Zhengzhou 450001, People's Republic of China
- (Received 9 November 2011; published 18 May 2012)

Using a data sample containing 1.06×10^8 ψ' events collected with the BESIII detector at the BEPCII electron-positron collider, we search for a light exotic particle X in the process $\psi' \rightarrow \pi^+ \pi^- J/\psi$, $J/\psi \rightarrow \gamma X$, $X \rightarrow \mu^+ \mu^-$. This light particle X could be a Higgs-like boson A^0 , a spin-1 U boson, or a pseudoscalar sgoldstino particle. In this analysis, we find no evidence for any $\mu^+ \mu^-$ mass peak between the mass threshold and $3.0 \text{ GeV}/c^2$. We set 90%-confidence-level upper limits on the product-branching fractions for $J/\psi \rightarrow \gamma A^0$, $A^0 \rightarrow \mu^+ \mu^-$ which range from 4×10^{-7} to 2.1×10^{-5} , depending on the mass of A^0 , for $M(A^0) < 3.0 \text{ GeV}/c^2$. Only one event is seen in the mass region below $255 \text{ MeV}/c^2$, and this has a $\mu^+ \mu^-$ mass of $213.3 \text{ MeV}/c^2$ and the product-branching-fraction upper limit 5×10^{-7} .

DOI: 10.1103/PhysRevD.85.092012

PACS numbers: 14.80.Da, 13.20.Gd, 13.66.Fg, 14.40.Pq

* Also at the Moscow Institute of Physics and Technology, Moscow, Russia

† On leave from the Bogolyubov Institute for Theoretical Physics, Kiev, Ukraine

‡ University of Piemonte Orientale and INFN (Turin)

§ Currently at INFN and University of Perugia, I-06100 Perugia, Italy

|| Also at the PNPI, Gatchina, Russia

¶ Now at Nagoya University, Nagoya, Japan

The fundamental nature of mass and dark matter remain among the great mysteries and challenges of science. The Higgs mechanism is a theoretically appealing way to account for masses of elementary particles [1]. A light Higgs-like pseudoscalar boson A^0 is predicted in the next-minimal supersymmetric extension of the standard model [2–4]. A neutral spin-1 boson U in the framework of the supersymmetric standard model extension is predicted to play an essential role in the annihilations of dark matter

[5–7]. Astrophysical observations by PAMELA [8] and ATIC [9] have been interpreted as being due to dark matter annihilation mediated by a light-gauge U boson [10] which couples to standard model particles. The HyperCP experiment [11] observed three anomalous $\Sigma^+ \rightarrow p\mu^+\mu^-$ events with $\mu^+\mu^-$ invariant mass clustered around $214.3 \text{ MeV}/c^2$ which are consistent with the process $\Sigma^+ \rightarrow pX$, $X \rightarrow \mu^+\mu^-$. A particle with these properties could be the pseudoscalar sgoldstino particle [12] in various supersymmetric models [13], a light pseudoscalar Higgs-like boson A^0 [14], or a vector U boson [15] as described above. The lifetime for the pseudoscalar particle case is estimated to be 10^{-14} s [16]; which for the U boson depends on the mass of the boson and is smaller than 10^{-14} s when the mass of the U boson is more than $100 \text{ MeV}/c^2$ [17].

The D0 [18], CMS [19], LEP [20], CLEO [21], BABAR [22,23], and Belle [24] experiments have searched for light dilepton-resonance production using data from $p\bar{p}$ collisions, e^+e^- collisions, and b -quark decays. No evidence for a signal of new physics has been found. It remains important to check the possibility that a particle of these types couples to the c -quark and leptons. The branching fraction of $J/\psi \rightarrow \gamma A^0$ is expected to be around the 10^{-9} to 10^{-7} level [4]. The only search for this kind of particle from charmonium decay was done by the Crystal Ball experiment where from fits to the γ recoil energy spectrum, they set branching fraction upper limits of $J/\psi \rightarrow \gamma A^0$ which are less than 1.4×10^{-5} (90% C.L.) for $M(A^0) < 1.0 \text{ GeV}/c^2$ [25].

The couplings of the Higgs to fermions are proportional to the fermion masses. For an A^0 boson with mass below the τ -pair threshold, the decay $A^0 \rightarrow \mu^+\mu^-$ is expected to be dominant. We use the process $\psi' \rightarrow \pi^+\pi^-J/\psi$, $J/\psi \rightarrow \gamma A^0$, $A^0 \rightarrow \mu^+\mu^-$ to search for an A^0 with the BESIII detector [26] at the BEPCII electron-positron collider [27]. This A^0 search is also sensitive to a light spin-1 U boson or a pseudoscalar sgoldstino particle. We assume the A^0 particle is a pseudoscalar (or scalar) particle which has narrow width and negligible decay time.

BEPCII is a double-ring e^+e^- collider with a design peak luminosity of $10^{33} \text{ cm}^{-2} \text{ s}^{-1}$. The BESIII detector is based on a large 1-Tesla solenoid magnet and covers 93% of the total 4π solid angle surrounding the e^+e^- collision point with four major detection systems:

- (i) A small-cell, helium-based main drift chamber with 43 layers which provide an average single-hit resolution of $135 \mu\text{m}$, charged-particle momentum resolution of 0.5% at $1 \text{ GeV}/c$, and a dE/dx resolution that is better than 6%.
- (ii) An electromagnetic calorimeter (EMC) consisting of 6240 CsI(Tl) crystals configured in a cylindrical structure (barrel) and two end caps. The energy resolution for 1.0 GeV γ rays is 2.5% in the barrel

and 5% in the end caps, and the position resolution is 6 mm in the barrel and 9 mm in the end caps.

- (iii) A time-of-flight system constructed of 5-cm-thick plastic scintillators, with 176 pieces of 2.4 m long counters arranged in a two-layer barrel and 96 fan-shaped counters in the end cap regions. The barrel (end cap) time resolution of 80 ps (110 ps) provides 2σ K/π separation for momenta up to $\sim 1.0 \text{ GeV}/c$.
- (iv) Muon identification is provided by 1000 m^2 of resistive plate chambers that are interspersed in the magnet's iron flux return (MUC). Nine barrel and eight end cap layers provide 2 cm position resolution for penetrating particles.

The analysis is based on 1.06×10^8 events collected at the peak of the ψ' resonance. The number of ψ' events was determined by counting inclusive hadronic events as described in Ref. [28] with an estimated uncertainty of 4%. Monte Carlo (MC) events are simulated with the GEANT4 program [29] and experimentally determined resolutions of the wires and counters in the detector.

For the event selection, we first require two positive and two negative charged tracks and at least one good photon. We also use μ identification information, veto π^0 s, place restrictions on the mass recoiling from the $\pi^+\pi^-$ system, and apply kinematic constraints. The dominant backgrounds are from $\psi' \rightarrow \pi^+\pi^-J/\psi$, with $J/\psi \rightarrow \gamma\pi^+\pi^-$, $J/\psi \rightarrow \rho\pi \rightarrow \pi^+\pi^-\pi^0$ or $J/\psi \rightarrow l^+l^-$. The kinematic constraints are especially effective for removing backgrounds from $J/\psi \rightarrow \pi^+\pi^-\pi^0$ and $J/\psi \rightarrow l^+l^-$ decays. A π^0 veto is used to reject $J/\psi \rightarrow \pi^+\pi^-\pi^0$ events. The selection requirements used for the π^0 veto, the $\pi^+\pi^-$ recoil mass requirement, and the kinematic fit quality are optimized for the assumption that the branching fraction for $J/\psi \rightarrow \gamma A^0$, $A^0 \rightarrow \mu^+\mu^-$ is at the 10^{-6} level and using $s/\sqrt{s+b}$ as a figure of merit, where s is the expected number of signal events and b is the number of background events. The track selection criteria are standard in BESIII analysis.

Candidate photons are energy clusters in the EMC which: (1) are within the fiducial region of the EMC ($|\cos\theta_\gamma| < 0.8$ for the barrel and $0.84 < |\cos\theta_\gamma| < 0.92$ for the end caps); (2) are more than 20 degrees away from the extrapolated position of the closest charged track; (3) have a pulse time that is consistent with being produced together with the charged-track candidates.

Charged-track candidates are required to originate from the interaction point, $V_{xy} = \sqrt{V_x^2 + V_y^2} < 1 \text{ cm}$, $|V_z| < 10 \text{ cm}$, where V_x , V_y , and V_z are the x , y , and z coordinates of the point of closest approach to the interaction point. The tracks are also required to be within the polar angle region $|\cos\theta| < 0.93$.

Candidate muons are charged tracks in the active area of the barrel MUC ($|\cos\theta| < 0.75$) with: momentum higher than $0.7 \text{ GeV}/c$; energy deposition in the EMC between

0.15 GeV and 0.26 GeV; E/p (EMC energy over main-drift-chamber momentum) less than 0.5; and at least three associated hit layers in the MUC. For tracks in the momentum range $0.8 \text{ GeV}/c < p < 1.15 \text{ GeV}/c$, the MUC penetration depth is required to be greater than $(70p - 40) \text{ cm}$ (p in GeV/c); for tracks with $p > 1.15 \text{ GeV}/c$, the penetration depth is required to be more than 41 cm. Tracks with momentum above $0.8 \text{ GeV}/c$ are removed if the fit to the MUC hits either fails or gives a poor fit result. The muon identification (PID) single-track efficiency is typically 65%, and the π fake rate is less than 5%/track.

If there are multiple photons with energy above 25 MeV, we reject the event if any pair of these photons has an invariant mass within $40 \text{ MeV}/c^2$ of m_{π^0} . For the multiphoton events that remain, the γ with the highest energy is selected as the photon used in the analysis. The pair of oppositely charged tracks with recoil mass closest to the J/ψ mass is assigned as the π^+ and π^- and the other two tracks as the μ^+ and μ^- . At least one of the tracks assigned as a muon is required to satisfy the μ -PID criteria. We select events with a $\pi^+\pi^-$ recoil mass in the range between $3.092 \text{ GeV}/c^2$ and $3.102 \text{ GeV}/c^2$ and perform a four-constraint energy-momentum conserving kinematic fit using the selected γ and four charged tracks. We require $\chi^2 < 40$ and $M(\mu^+\mu^-) < 3.02 \text{ GeV}/c^2$.

Simulations where the A^0 width is set to zero and the mass is set at 71 different values which range from $0.212 \text{ GeV}/c^2$ to $3.0 \text{ GeV}/c^2$ indicate that the selection efficiency varies between 28% and 18%, depending on the mass of A^0 , as shown in Fig. 1(a). The simulation is done for $1 \text{ MeV}/c^2$ A^0 mass steps for $M(A^0)$ between $0.212 \text{ GeV}/c^2$ to $0.22 \text{ GeV}/c^2$, $5 \text{ MeV}/c^2$ steps for $M(A^0)$ between $0.22 \text{ GeV}/c^2$ to $0.4 \text{ GeV}/c^2$ and $100 \text{ MeV}/c^2$ steps for $M(A^0)$ above $0.4 \text{ GeV}/c^2$. We fit the resulting efficiency values piecewise with second-order polynomial shapes to get the A^0 -mass-dependent efficiency which includes any bias caused by the fit. The A^0 mass resolution determined from the MC simulation increases

with A^0 mass, ranging from $0.1 \text{ MeV}/c^2$ near the low-mass threshold to about $5 \text{ MeV}/c^2$ for masses near $3.0 \text{ GeV}/c^2$. The efficiencies for spin-1 U production are the same as those for the A^0 to within a few percent.

The $\mu^+\mu^-$ mass distribution of selected data events is shown in Fig. 2(a). Over the entire mass range, from threshold to $3.0 \text{ GeV}/c^2$, there is no evident narrow peak. Below $255 \text{ MeV}/c^2$, there is only one event, with $\mu^+\mu^-$ invariant mass of $213.3 \text{ MeV}/c^2$. The expected A^0 mass resolution is about $0.2 \text{ MeV}/c^2$ for $M(A^0) = 213.3 \text{ MeV}/c^2$, and the major background in this region comes from $\psi' \rightarrow \pi^+\pi^-J/\psi$, $J/\psi \rightarrow \gamma\pi^+\pi^-$. The expected number of background events in the mass region near $213.3 \text{ MeV}/c^2$ is about $0.2/\text{MeV}/c^2$; the observation of one event in this region is consistent with that at background level.

To set upper limits on the production rates for different masses, we do unbinned maximum-likelihood fits to $\sim 300 \text{ MeV}/c^2$ -wide ranges of the $\mu^+\mu^-$ invariant mass spectrum where the mass of the A^0 peak is restricted to be within a series of $5 \text{ MeV}/c^2$ -wide intervals near the center of the range. In each fit, we use a MC-determined shape for the A^0 signal, and for the background shape, we use a polynomial. We do not find any significant signal and set Bayesian upper limits on the signal yield in each $5 \text{ MeV}/c^2$ interval. Figure 1(b) shows a typical fit to the $\mu^+\mu^-$ invariant mass spectrum in the $5 \text{ MeV}/c^2$ -wide interval centered at $2.43 \text{ GeV}/c^2$.

We use different fit ranges, polynomial background shapes of different orders, and MC signal shapes for different A^0 mass values to estimate the fit-related systematic error on the signal yield in each mass interval. We first fit using the MC signal shape from the nearest generated A^0 mass for the signal shape with a second-order polynomial to represent the background shape. We then increase and decrease the edges of fit range by $\pm 5 \text{ MeV}/c^2$, use signal shapes from the MC fits that are one step lower and one step higher than the nearest one, and use first- and third-order polynomial shapes for the background. Each fit is required to converge. For each mass interval, the fit

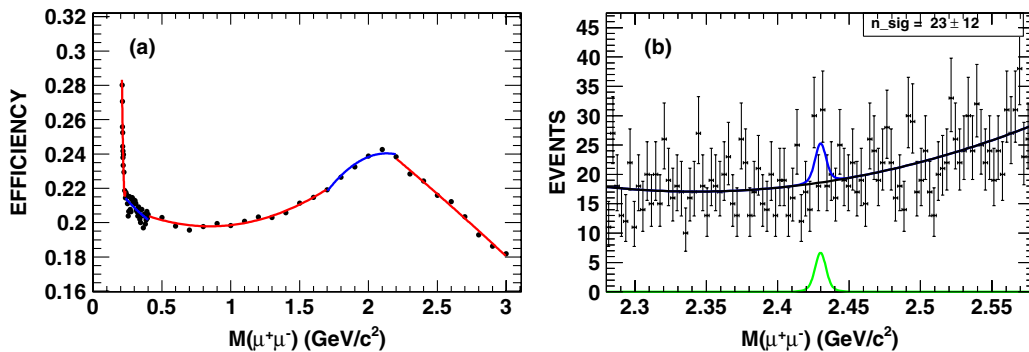


FIG. 1 (color online). (a) The event selection efficiency for $\psi' \rightarrow \pi^+\pi^-J/\psi$, $J/\psi \rightarrow \gamma A^0$, $A^0 \rightarrow \mu^+\mu^-$; (b) The fit to the invariant-mass spectrum $M(\mu^+\mu^-)$ in the $5 \text{ MeV}/c^2$ wide interval centered at $2.43 \text{ GeV}/c^2$ showing the total fit result and the background-subtracted signal.

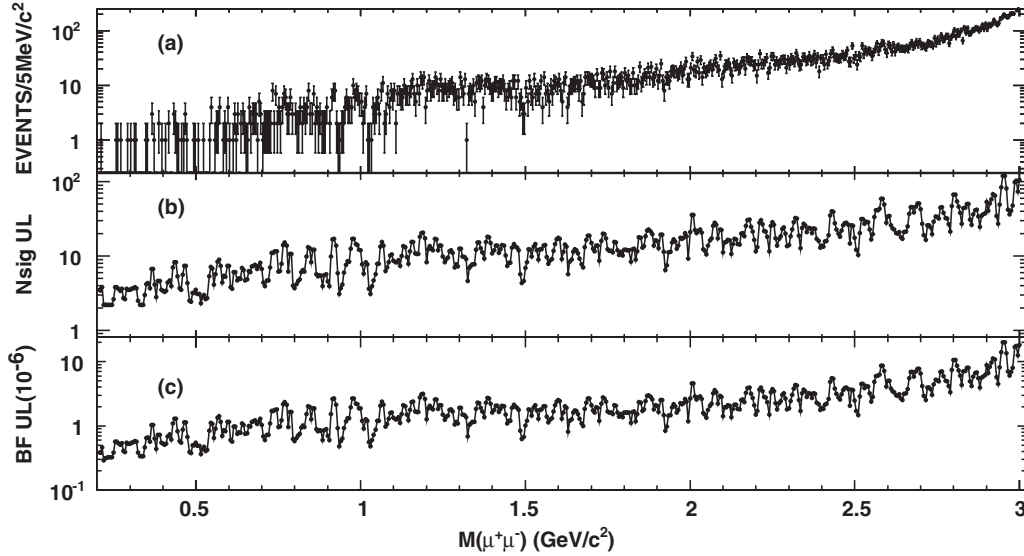


FIG. 2. (a) The $\mu^+ \mu^-$ invariant-mass spectrum for the selected $\psi' \rightarrow \pi^+ \pi^- J/\psi$, $J/\psi \rightarrow \gamma \mu^+ \mu^-$ events; (b) 90% C.L. upper limits on the number of signal events (Nsig UL) as a function of the $\mu^+ \mu^-$ invariant mass; (c) upper limits on the branching fractions (BF UL) for $J/\psi \rightarrow \gamma A^0$, $A^0 \rightarrow \mu^+ \mu^-$ at the 90% C.L.

variation that produces the largest number of signal events is used to determine the 90% C.L. upper limits, which are shown in Fig. 2(b).

The systematic errors in the $J/\psi \rightarrow \gamma A^0$, $A^0 \rightarrow \mu^+ \mu^-$ product-branching-fraction measurement are summarized in Table I; these include contributions from tracking, particle identification, photon selection, kinematic fit, $\pi^+ \pi^-$ recoil mass requirement, and π^0 veto. The uncertainty of the number of ψ' events is 4% [28], and that of the $\psi' \rightarrow \pi^+ \pi^- J/\psi$ branching fraction is 1.2% [30].

The uncertainty due to data-MC differences in the charged-tracking efficiency is 1% per track and added linearly. This is determined from high-statistics, low-background samples of $J/\psi \rightarrow \rho \pi$ and $J/\psi \rightarrow p \bar{p} \pi^+ \pi^-$ events. In this analysis, there are four charged tracks, and the relative systematic error is 4%.

The uncertainty due to the photon reconstruction is determined to be 1% for each photon using three different

methods as described in Ref. [31]. These include a missing photon and π^0 decay angle method using a clean sample of $\psi' \rightarrow \pi^+ \pi^- J/\psi$, $J/\psi \rightarrow \rho^0 \pi^0$ events, and a missing π^0 method using $\psi' \rightarrow \pi^0 \pi^0 J/\psi$, $J/\psi \rightarrow l^+ l^-$ events.

The uncertainties due to muon identification are determined from studies of a sample of radiative muon pair events that contain one photon. We determine muon PID probabilities for 0.3 GeV/c steps in track momentum and determine that the efficiency is about 65% per track; the data-MC differences in efficiency are less than 4% per track. Since we require only one muon to satisfy the identification criteria, the PID-related systematic error is less than 2.5%.

The systematic uncertainty associated with the kinematic fit is determined by applying a similar kinematic fit to MC and data samples of $\psi' \rightarrow \pi^+ \pi^- J/\psi$, $J/\psi \rightarrow \pi^+ \pi^- \pi^0$, $\pi^0 \rightarrow \gamma \gamma$ events. In the event selection for this study, if there are more than two candidate γ s, we use the most energetic γ together with the one that has the best one-constraint fit to $\pi^0 \rightarrow \gamma \gamma$. From data-MC differences for these events, the systematic error associated with the kinematic fit is determined to be 3.2%.

It is unlikely for signal events to have an $M(\gamma \gamma)$ value that is near $m_{\pi^0}^0$; the efficiency reduction caused by the π^0 veto is less than 3%. The systematic error associated with the π^0 veto is studied with samples of $\psi' \rightarrow \gamma \chi_{cJ} \rightarrow \gamma \phi \phi \rightarrow \gamma 2(K^+ K^-)$ and $\psi' \rightarrow \pi^+ \pi^- J/\psi$, $J/\psi \rightarrow \gamma f_2(1270)$, $f_2(1270) \rightarrow \pi^+ \pi^-$ events from both MC simulation and data. From $\psi' \rightarrow \gamma \chi_{cJ} \rightarrow \gamma \phi \phi$, we determine the effect of the π^0 veto cut on the efficiency. For the second sample, we fit the $\pi^+ \pi^-$ mass spectrum to get the number of $f_2(1270) \rightarrow \pi^+ \pi^-$ events with and without the π^0 veto cut. Data and MC efficiency differences for the

TABLE I. The individual contributions to the total relative systematic error (%) in the product-branching-fraction measurement.

Source	Error
Tracking efficiency	4.0
Particle identification	2.5
Kinematic fit	3.2
γ efficiency	1.0
$\pi^+ \pi^-$ recoil mass	1.2
π^0 veto	2.0
Number of ψ' s	4.0
$\mathcal{B}(\psi' \rightarrow \pi^+ \pi^- J/\psi)$	1.2
Total	7.5

π^0 veto are found to be less than 1.7% from the first channel and less than 2.0% from the second channel. We use 2% as the systematic error due to the $M(\gamma\gamma)$ requirement.

The systematic error caused by the $\pi^+\pi^-$ recoil mass requirement is analyzed with the sample of $\psi' \rightarrow \pi^+\pi^-J/\psi$, $J/\psi \rightarrow \mu^+\mu^-$ events in the data and from MC simulation. From the numbers of events with and without the recoil mass requirement, we determine data and MC efficiency difference to be less than 1.2%.

The systematic errors are summarized in Table I; each of these are the largest errors over the entire $M(\mu^+\mu^-)$ range. Assuming the errors from all sources are independent, the total error is determined from the quadrature sum to be 7.5%.

We determine the upper limit on the branching fractions of $J/\psi \rightarrow \gamma A^0$, $A^0 \rightarrow \mu^+\mu^-$ from the relation

$$\mathcal{B} < \frac{\text{Nsig(UL)}/\varepsilon}{N(\psi') \times \mathcal{B}(\psi' \rightarrow \pi^+\pi^-J/\psi) \times (1 - \sigma)}, \quad (1)$$

where Nsig(UL), shown in Fig. 2(b), is the upper limit on the number of signal events in each $M(\mu^+\mu^-)$ bin after consideration of the mass fitting systematic errors; ε is the A^0 -mass-dependent selection efficiency determined from MC simulation; $N(\psi') = 1.06 \times 10^8$ is the number of ψ' events [28]; and $\mathcal{B}(\psi' \rightarrow \pi^+\pi^-J/\psi) = (33.6 \pm 0.4)\%$ is the world average [30]. The upper limit is increased by a factor of $1/(1 - \sigma)$, where σ is the total systematic error (7.5%) to give a conservative result. The resulting $\mathcal{B}(J/\psi \rightarrow \gamma A^0) \times \mathcal{B}(A^0 \rightarrow \mu^+\mu^-)$ upper-limit values range from 4×10^{-7} for an A^0 mass near threshold to 2.1×10^{-5} for $M(A^0)$ near $3.0 \text{ GeV}/c^2$ and is shown in Fig. 2(c). The branching fraction upper limit is less than 10^{-6} for all $M(A^0)$ values below $0.36 \text{ GeV}/c^2$ and is less than 10^{-5} for all masses below $2.79 \text{ GeV}/c^2$.

In summary, we have searched for a light exotic particle at BESIII. No evidence is observed, and upper limits on the product-branching fractions for $J/\psi \rightarrow \gamma A^0$, $A^0 \rightarrow \mu^+\mu^-$ range from 4×10^{-7} to 2.1×10^{-5} , depending on the mass of the A^0 , are established. These limits are new stringent experimental results from charmonium decays and can rule out much of the parameter space in theoretical models [32]. Only one event is observed in the low-mass region below $255 \text{ MeV}/c^2$, with a $\mu^+\mu^-$ mass of $213.3 \text{ MeV}/c^2$. For $M(A^0) < 255 \text{ MeV}/c^2$, including the $214.3 \text{ MeV}/c^2$ mass value of the anomalous HyperCP $\Sigma^+ \rightarrow p\mu^+\mu^-$ events, the product-branching-fraction upper limit is 5×10^{-7} at the 90% C.L. Although these branching fraction upper limits are computed for a spin-0 particle, they are the same, to within a few percent, for a spin-1 particle.

The BESIII Collaboration thanks the staff of BEPCII and the computing center for their hard efforts. This work is supported in part by the Ministry of Science and Technology of China under Contract No. 2009CB825200; National Natural Science Foundation of China (NNSFC) under Contract Nos. 10625524, 10821063, 10825524, 10835001, 10935007; Joint Funds of the National Natural Science Foundation of China under Contract No. 11079008; the Chinese Academy of Sciences (CAS) Large-Scale Scientific Facility Program; CAS under Contract Nos. KJCX2-YW-N29, KJCX2-YW-N45; 100 Talents Program of CAS; Istituto Nazionale di Fisica Nucleare, Italy; U. S. Department of Energy under Contract Nos. DE-FG02-04ER41291, DE-FG02-91ER40682, DE-FG02-94ER40823; U. S. National Science Foundation; University of Groningen (RuG) and the Helmholtzzentrum fuer Schwerionenforschung GmbH (GSI), Darmstadt; WCU Program of National Research Foundation of Korea under Contract No. R32-2008-000-10155-0.

-
- [1] P. W. Higgs, *Phys. Rev. Lett.* **13**, 508 (1964).
 [2] R. Dermisek and J. F. Gunion, *Phys. Rev. Lett.* **95**, 041801 (2005).
 [3] R. Dermisek and J. F. Gunion, *Phys. Rev. D* **77**, 015013 (2008).
 [4] R. Dermisek, J. F. Gunion, and B. McElrath, *Phys. Rev. D* **76**, 051105 (2007).
 [5] P. Fayet, *Phys. Lett. B* **95**, 285 (1980).
 [6] C. Boehm and P. Fayet, *Nucl. Phys. B* **683**, 219 (2004).
 [7] P. Fayet, *Phys. Rev. D* **74**, 054034 (2006).
 [8] O. Adriani *et al.* (PAMELA Collaboration), *Nature (London)* **458**, 607 (2009).
 [9] J. Chang *et al.* (ATIC Collaboration), *Nature (London)* **456**, 362 (2008).
 [10] M. Pospelov, A. Ritz, and M. B. Voloshin, *Phys. Lett. B* **662**, 53 (2008); N. Arkani-Hamed and N. Weiner, *J. High Energy Phys.* **12** (2008) 104.
 [11] H. K. Park *et al.* (HyperCP Collaboration), *Phys. Rev. Lett.* **94**, 021801 (2005).
 [12] D. S. Gorbunov and V. A. Rubakov, *Phys. Rev. D* **73**, 035002 (2006).
 [13] J. Ellis, K. Enqvist, and D. Nanopoulos, *Phys. Lett. B* **147**, 99 (1984); T. Bhattacharya and P. Roy, *Phys. Rev. D* **38**, 2284 (1988); G. Giudice and R. Rattazzi, *Phys. Rep.* **322**, 419 (1999).

- [14] X. G. He, J. Tandean, and G. Valencia, *Phys. Rev. Lett.* **98**, 081802 (2007).
- [15] M. Reece and L. T. Wang, *J. High Energy Phys.* **07** (2009) 051; M. Pospelov, *Phys. Rev. D* **80**, 095002 (2009); C. H. Chen, C. Q. Geng, and C. W. Kao, *Phys. Lett. B* **663**, 400 (2008).
- [16] C. Q. Geng and Y. K. Hsiao, *Phys. Lett. B* **632**, 215 (2006).
- [17] P. Fayet, *Nucl. Phys. B* **187**, 184 (1981).
- [18] V. M. Abazov *et al.* (D0 Collaboration), *Phys. Rev. Lett.* **103**, 061801 (2009).
- [19] S. Chatrchyan *et al.* (CMS Collaboration), *J. High Energy Phys.* **07** (2011) 098.
- [20] S. Schael *et al.* (ALEPH Collaboration), *J. High Energy Phys.* **05** (2010) 049.
- [21] W. Love *et al.* (CLEO Collaboration), *Phys. Rev. Lett.* **101**, 151802 (2008).
- [22] B. Aubert *et al.* (BABAR Collaboration), *Phys. Rev. Lett.* **103**, 081803 (2009).
- [23] B. Aubert *et al.* (BABAR Collaboration), *Phys. Rev. Lett.* **103**, 181801 (2009).
- [24] H. J. Hyun *et al.* (Belle Collaboration), *Phys. Rev. Lett.* **105**, 091801 (2010).
- [25] C. Edwards *et al.* (Crystal Ball Collaboration), *Phys. Rev. Lett.* **48**, 903 (1982).
- [26] M. Ablikim *et al.* (BESIII Collaboration), *Nucl. Instrum. Methods Phys. Res., Sect. A* **614**, 345 (2010).
- [27] J. Z. Bai *et al.* (BES Collaboration), *Nucl. Instrum. Methods Phys. Res., Sect. A* **344**, 319 (1994); **458**, 627 (2001).
- [28] M. Ablikim *et al.* (BESIII Collaboration), *Phys. Rev. D* **81**, 052005 (2010).
- [29] S. Agostinelli *et al.* (GEANT4 Collaboration), *Nucl. Instrum. Methods Phys. Res., Sect. A* **506**, 250 (2003).
- [30] K. Nakamura *et al.* (Particle Data Group), *J. Phys. G* **37**, 075021 (2010).
- [31] M. Ablikim *et al.* (BESIII Collaboration), *Phys. Rev. D* **83**, 112005 (2011).
- [32] P. Fayet, *Phys. Lett. B* **675**, 267 (2009).